Fisheries and Oceans Canada | Pêches et Océans Canada
Ecosystems and Oceans Science | Sciences des écosystèmes et des océans

Canadian Science Advisory Secretariat (CSAS)

Research Document 2024/046

Québec Region

Time-Space Distribution of North Atlantic Right Whale in Gulf of St. Lawrence from Acoustic Monitoring between 2010 and 2022

Y. Simard, S. Giard, N. Roy, P. Royer, M.-E., Chartrand-Lemieux, and E. Perreault

Maurice Lamontagne Institute
Fisheries and Oceans Canada
850 route de la mer
Mont-Joli, QC, G5H 3Z4

September 2024

Foreword

This series documents the scientific basis for the evaluation of aquatic resources and ecosystems in Canada. As such, it addresses the issues of the day in the time frames required and the documents it contains are not intended as definitive statements on the subjects addressed but rather as progress reports on ongoing investigations.

Published by:

Fisheries and Oceans Canada
Canadian Science Advisory Secretariat
200 Kent Street
Ottawa ON K1A 0E6

http://www.dfo-mpo.gc.ca/csas-sccs/
csas-sccs@dfo-mpo.gc.ca

ISSN 1919-5044
ISBN 978-0-660-73270-1 Cat. No. Fs70-5/2024-046E-PDF

Correct citation for this publication:

Simard, Y., Giard, S., Roy, N., Royer, P., Chartrand-Lemieux, M.-E., and Perreault, E. 2024. Time-Space Distribution of North Atlantic Right Whale in Gulf of St-Lawrence from Acoustic Monitoring between 2010 and 2022. DFO Can. Sci. Advis. Sec. Res. Doc. 2024/046. vi + 26 p.

Aussi disponible en français :

Simard, Y., Giard, S., Roy, N., Royer, P., Chartrand-Lemieux, M.-E., et Perreault, E. 2024. Répartition spatio-temporelle de la baleine noire de l'Atlantique Nord dans le golfe du Saint-Laurent selon les données de surveillance acoustique enregistrées entre 2010 et 2022. Secr. can. des avis sci. du MPO. Doc. de rech. 2024/046. vi + 27 p.

TABLE OF CONTENTS

LIST OF FIGURES

LIST OF TABLES

ABSTRACT

Recordings from the passive acoustic monitoring (PAM) network deployed in the Estuary and Gulf of St. Lawrence for detecting marine mammals and assessing ocean noise are analyzed to extract the time-space pattern of habitat use by North Atlantic right whale (NARW) from 2010 to 2022. Data from an ensemble of 24 027 days of observation, recorded at 12 seafloor PAM stations and 8 ocean observing (OOS) buoys, were processed to detect NARW upcalls using an artificial intelligence (AI) algorithm previously developed for this ecosystem.

NARW occurrences in this marginal inland sea of the Northwest Atlantic during the ice-free period, shifted in 2015 from occasional to frequent. High occurrence levels were maintained since. Although NARW upcalls were detected over a large part of the Gulf, they were very rare out of the southern Gulf shelf and north-northwest of Anticosti Island.

Excluding rare presence events, the average occurrence season began at the end of April and ended at the beginning of December. The majority of annual occurrences (90% of occurrence days) was between 5 June and 2 November. The NARW occurrences into the Gulf from our PAM network culminated in mid-August. The established general spatial pattern then persisted until November. It comprised two main areas: the Southwestern shelf of the Gulf of St. Lawrence, where most of the occurrences were observed, and the area north-northwest of Anticosti Is., where the occurrence levels were lower. The occurrences in Shediac trough dominated throughout the season. Variability of occurrences at the stations within and between season was common. The proportion of seasonal occurrence in the Gulf throughout the season is analyzed to infer the seasonal mean pattern of NARW incursion and retreat, and to extract relevant dates for NARW protection and management decisions.

INTRODUCTION

From spring to winter, since 2015, the Gulf of St. Lawrence is used as seasonal foraging ground by a large proportion of the endangered (Cooke 2020; COSEWIC 2013; DFO 2014) North Atlantic right whale (NARW) population (Simard et al. 2019), which presently counts ~ 350 individuals (Linden 2023). Mark-recapture analysis for 2015-2019 (Crowe et al. 2021) estimated that ~ 40% of the population now use this part of their life domain in North Atlantic, pushing northward their usual main distribution and seasonal movements (Brillant et al. 2015; Davis et al. 2017; DFO 2014; Kraus and Rolland 2007; Winn et al. 1986). The high inter-annual return rate of the same individuals indicate a high degree of seasonal fidelity of this fraction of the NARW population to the Gulf of St. Lawrence, with individual residencies extending up to 5 months (Crowe et al. 2021). The seasonal occurrences from PAM observations from 2015 to 2018 tended to increase from June to September, before decreasing during fall, with rare occurrences after December (Simard et al. 2019). This general temporal pattern was also noted for the seasonal growth of the NARW individual discovery curves and the monthly cumulated number of individuals, with the seasonal arrival of animals completed by the end of August (Crowe et al. 2021). The bulk of passive acoustic monitoring (PAM) NARW detections from 2015 to 2018 was found over the Southwestern Gulf shelf, between Gaspé and Cabot strait (Simard et al. 2019), but some areas of the Gulf were then poorly covered by the coarse network of PAM stations. Following the 2017 NARW high-mortality event in the Gulf (Daoust et al. 2017), the DFO NARW PAM effort was enhanced with the addition of year-round stations of bottom-mounted hydrophones and a set of real-time ocean observing systems (OOS) equipped with NARW PAM detectors operating during the ice-free period. The present report contributes the new information brought by this DFO PAM observation network in tracking the spatial-temporal use pattern of the Gulf of St. Lawrence by NARW since 2010. It complements other efforts to track the evolution of this singular large-scale event over the Northwest Atlantic that is forcing distributional changes of this small NARW population, through a warming trend that is affecting their preferred prey (Davis et al. 2017; Meyer-Gutbrod et al. 2021; Plourde et al. 2019; Record et al. 2019; Roberts et al. 2024).

METHODS

PAM NETWORK DEPLOYED FROM 2010 TO 2022

The data ensemble analyzed in the present work was collected by a network of PAM stations that was progressively densified throughout the 12-year period. It is made up of two datasets that differ by their recording setups. The first set includes 12 stations, where the instruments were deployed a few meters above the seafloor following usual I-type oceanographic moorings, with an anchor, an acoustic release, the autonomous hydrophone system, and subsurface floats (Figure 1, stars, scheme, Table 1). The second set counts 8 stations, where the hydrophone was connected to a real-time and archiving Viking ocean observing system (OOS) surface buoy anchored to the seafloor, with a 60-m long electro-mechanic cable providing power and transmission of the digital acoustic data. This latter cable was floating at the surface for half of its length before plunging towards the weighted hydrophone at a nominal depth of ~25 m (Figure 1, circles, photo, Table 2)

The 3D locations of the seafloor mounted PAM stations were optimized as much as possible to: 1) get the hydrophone within the regional sound channel, resulting from the presence of the cold intermediate layer (CIL) of the Gulf of St. Lawrence (cf. Galbraith et al. 2023); 2) minimize the risk of accidental damage by the northern shrimp bottom trawl fishery; 3) maximize the signal-to-noise ratio, by distancing the station position from the large imprint of the noisy shipping

routes crossing the Gulf (Aulanier et al. 2021), which drastically reduces the detection range of NARW upcalls from non-directional acoustic systems (cf. Gervaise et al. 2019a, 2019b; Gervaise et al. 2021; Simard et al. 2019; Simard et al. 2022); 4) account for the expected baleen whale feeding grounds, their migration corridors, and form a coarse grid that entirely covers the Gulf and Lower Estuary.

In 2019, the needs for quasi real-time continuous information on NARW presence for the triggering of protection measures from DFO and Transport Canada (TC) in different critical areas motivated the idea of harnessing the OOS Viking buoy network operating in the Gulf for oceanographic monitoring. An intelligent acoustic component was added to detect NARW upcalls and transmit the information in quasi real-time. All acoustic data were also simultaneously stored on the hydrophone and the OOS memories. The analysis presented in this report uses these latter, more complete, archived recordings compared to the OOS processed data that were subject to frequent interrupts. The locations of the OOS buoys were chosen based on the oceanographic monitoring objectives, but several of them were favorably placed for NARW passive acoustic monitoring. A few acoustic-only buoys were added in order to densify the network and cover other areas of expected NARW prey aggregation. On the OOS buoys, the targeted hydrophone depth of ~ 25 m did not reach the core of the CIL sound channel, but only its upper boundary below the summer thermocline. The horizontal distance from the buoy sought for the hydrophone was 30 m. However, actual depths and distances varied from the targets in response to currents and meteorological forcings.

The acoustic data acquisition used 4 different systems having relatively similar sensitivity characteristics for recording in the low frequency (LF) bandwidth of the NARW upcall (Table 3, Appendix 1, Figure 11). At the seafloor stations, the data acquisition included hourly sleep periods whose duration was selected to maximize the recorded acoustic bandwidth and the duration of the recording period between the biannual or annual services. At the Viking OOS stations, the recording was continuous and covered only the ice-free period, from the end of May or beginning of June to November.

PAM DATA ANALYSIS

The recorded signal was first down-sampled to 1000 samples/s, hence covering a [0-500 Hz] acoustic band, before being processed for detecting NARW upcalls, whose main acoustic band is between ~100 Hz and ~200 Hz (Parks and Tyack 2005; Parks et al. 2009) (cf. Appendix 1). The detection was then made using an upgraded version (Ver. 2.0) of the convoluted deep neural network (CDNN) AI-algorithm developed from a Gulf of St. Lawrence training dataset (5 962 samples) recorded with the same apparatus and settings as the present study and 3 000 samples from the Atlantic (DCLDE 2013) (Kirsebom et al. 2020, Table 2). The Ver. 2.0 of the CDNN AI-algorithm was trained with a larger dataset, by adding 14 693 samples from the Gulf of St. Lawrence for a total of 23 655 samples. Using a detection threshold of 0.7, the recall index (R= 0.73) of this Ver. 2.0 of the algorithm was enhanced by 3% and the precision index (P= 0.92) by 7% compared to Ver 1.0, when tested on the same series of fifty 30-min continuous data files (Kirsebom et al. 2020, Fig. 8; Appendix 2). All detected NARW upcalls were then validated by one trained expert, with confirmation by a second expert for doubtful cases, notably when humpback songs occurred (cf. Appendix 3), and false detections were eliminated.

Metrics

Let us define the binary indices $d_n(s, j)$ as the days with NARW upcall occurrence and $d_o(s, j)$ as the days of observation, where s = 1*,* 2*, ...*12*, A,B, ...H* is the station and j =1*,* 2*, ...,*N_d spans all days of the time series.

Defining $d_7(s,w)$ as the number of days with NARW upcalls at station s within a week w, and j_w as the days falling within the week w, the index for the time series (Figures 2 and 3) is constructed as :

$$d_7(s,w) = \sum_{j_w=1}^{7} d_n(s,j_w) \tag{1}$$

To analyze the importance of NARW occurrence at various space and time scales, the quantity adopted in this report is the *proportion of observation days where NARW upcalls are detected (p_n)*. According to the scale of interest, the data is partitioned in space (s) and time (j), and the total number of days of occurrence (d_n) and observation (d_o) are summed within each partition group to get the proportion.

Taking a partition in space R (eg. region or group of stations (Viking or seafloor PAM stations)), and a partition in time T (eg. Julian days, months), $p_n(R, T)$ is given by :

$$p_n(R,T) = \frac{\sum_{s\in R}\sum_{j\in T} d_n(s,j)}{\sum_{s\in R}\sum_{j\in T} d_o(s,j)} \tag{2}$$

To build the maps of figure 7 to 9, R is taken as a single station and T consists of all Julian days falling within the month $m(j_m)$ (all years (y) included) :

$$p_n(s,m) = \frac{\sum_{y=2015}^{2022}\sum_{j_m\in m} d_n(s,y,j_m)}{\sum_{y=2015}^{2022}\sum_{j_m\in m} d_o(s,y,j_m)}\text{ , (seafloor PAM)} \tag{3a}$$

$$p_n(s,m) = \frac{\sum_{y=2019}^{2022}\sum_{j_m\in m} d_n(s,y,j_m)}{\sum_{y=2019}^{2022}\sum_{j_m\in m} d_o(s,y,j_m)}\text{ , (Viking buoys)} \tag{3b}$$

For the central curves of figures 4 and 5, all stations of a particular type (Viking buoys or seafloor PAM) are included, and the time dimension is partitioned monthly (all years included):

$$p_n(R,m) = \frac{\sum_{s\in R}\sum_{y=2015}^{2022}\sum_{j_m\in m} d_n(s,y,j_w)}{\sum_{s\in R}\sum_{y=2015}^{2022}\sum_{j_m\in m} d_o(s,y,j_w)}\text{, (seafloor PAM)} \tag{4a}$$

$$p_n(R,m) = \frac{\sum_{s\in R}\sum_{y=2019}^{2022}\sum_{j_m\in m} d_n(s,y,j_w)}{\sum_{s\in R}\sum_{y=2019}^{2022}\sum_{j_m\in m} d_o(s,y,j_w)}\text{, (Viking buoys)} \tag{4b}$$

whereas the extent of the variation across the years is shown by taking the extrema (with respect to y) of :

$$p_n(R,y,m) = \frac{\sum_{s\in R}\sum_{j_m\in m} d_n(s,y,j_w)}{\sum_{s\in R}\sum_{j_m\in m} d_o(s,y,j_w)}. \tag{5}$$

And similarly for figure 6, where the R's are defined according to geographic regions of interest.

Finally, figure 10 includes only the seafloor PAM stations from 2015 to 2022 and days are grouped according to Julian day (irrespective of the year):

$$p_n(j) = \frac{\sum_{s=1}^{12}\sum_{y=2015}^{2022} d_n(s,y,j)}{\sum_{s=1}^{12}\sum_{y=2015}^{2022} d_o(s,y,j)}. \tag{6}$$

and the latter is then normalized to sum to 1.0 :

$$pn_n(j) = \frac{p_n(j)}{\sum_{j=1}^{366} p_n(j)}. \tag{7}$$

The corresponding normalized distribution of days of observation per Julian day is given by:

$$pn(j) = \frac{\sum_{s=1}^{12}\sum_{y=2015}^{2022} d_0(s,y,j)}{\sum_{j=1}^{366}\sum_{s=1}^{12}\sum_{y=2015}^{2022} d_0(s,y,j)}\,. \tag{8}$$

RESULTS

ACOUSTIC OBSERVATION EFFORT AND OCCURRENCE RATIOS

The number of days with PAM observation at the 12 seafloor stations from 2010 to 2022 varied from 353 days to 4,391 days (1). Summing over all stations and years, the number of days with observations represents a challenging big-data processing task containing 24,027 days of acoustic recordings. The number of days with NARW upcall occurrence at the 12 stations varied from 0 to 534 days. The corresponding percentage of days with NARW upcall occurrence varied from 0% to 25%. It exceeded 1% at only 6 of the 12 stations; 5 of them (stations 2-6) were located in the Southwest Gulf and adjacent southern shelf of the Laurentian Channel, and the other one (station 11) was located on the northern slope of the ~200-m deep basin, northwest of Anticosti Is. (Figure 1). Two (2) of the other 6 stations had rare NARW upcall occurrences, and none were detected at 4 stations (stations 7, 9, 10, and 12). Despite their rare occurrence, these few dispersed NARW detections indicate that NARW presence was noted out of the frequently visited areas during the observation period.

The observations with the Viking OOS buoys for ~7 months per year (winter excluded) started only in 2019. The number of days with PAM effort among the 8 stations varied from 114 to 663 (Table 2). The cumulated number of observation days over all stations from 2019 to 2022 was 3,413. The percentage of days with NARW upcall detection at the stations varied from 2.2 to 51.8. These later proportions are higher than for the seafloor PAM stations, partly because the sampling season focused on the seasonal frequent NARW occurrence period and areas.

NARW UPCALL OCCURRENCE TIME SERIES AT THE STATIONS

The NARW upcall occurrence time series at the stations indicate that the high level of frequentation of the Gulf of St. Lawrence after 2015 reported by Simard et al. (2019) continued up to 2022 (Figure 2, Figure 3). Stations with steady occurrences during the ice-free period were those located in the Southwest Gulf (stations 3-5, E-F). The later were aligned along the Shediac trough, from its mouth, on southern slope of the Laurentian Channel, to its head off Shediac peninsula (Figure 1). The seasonal occurrence patterns at the stations varied across years, for both the stations with steady occurrence (e.g. stations 4, 6, E-F) and those less frequented (e.g. stations 3, 11, A, C, G). This spatial-temporal variability within season and across years indicates a general behavior of prolonged stays in particular areas, mixed with mesoscale (> ~25 km) displacements.

The year-round proportion of days with NARW upcall occurrences per month at the stations of frequent occurrence summarizes the general time-space annual pattern since 2015 (Figure 4, Figure 5, Figure 6). For both datasets, average seasonal occurrences were highest at stations at the head of the Shediac trough (stations 4, E) and their growth tended to start and peak ~1-2 month earlier than at the stations closer to the Laurentian channel (stations 2, 3, 6, F). The occurrences at the three stations on the Southern Gulf shelf, east of the Shediac trough, stations B-D, seemed to peak at about the same time as for stations 4 and E, or with slight delay, but their more recent deployment makes the comparison uncertain. The low but recurrent occurrences at station 2, on the Laurentian Channel slope, east of the Magdalen Is., start as early as April but their maxima occur later in summer and fall. Similarly, the occurrences at the southernmost station, half-way between Prince-Edward Is. and Magdalen Is., station A, were higher from August to October. The 2-month high-frequentation period between August and October at other two stations with notable occurrences, Northern Gulf stations 11 and G, and appeared to be delayed by ~ 1 month from that of the Southern Gulf stations (Figure 6).

MONTHLY MAPS OF NARW UPCALL OCCURRENCE

The maps of the average proportion of days with NARW upcall occurrence per month at the stations for 2015 to 2022 summarizes the seasonal distribution pattern (Figure 7, Figure 8, Figure 9). A few detections occur as early as April (Figure 7, April arrows), especially in Southwestern Gulf, and in May, the average proportion of days with NARW upcall occurrences reaches 20% at 2 stations (Figure 7, Figure 8, May). NARW are then also detected at the western point of Anticosti Is. (Figure 8, May). A similar occurrence pattern is observed in June while the proportion of occurrence days exceeds 70% at the head of Shediac trough (Figure 7, Figure 8, June). In July, the proportions of occurrence days at the stations increase by ~10 to 20%; station G West of Anticosti Island attains 10%, and Shediac trough head makes 90% (Figure 7, Figure 8, July). In August, the seasonal occurrence peaks; the proportion of occurrence days at stations in the Southwestern shelf exceeds 90%, station 11 northwest of Anticosti Is. gets its first occurrences with proportion of occurrence levels of almost 20% , and occurrence raises at station A between Prince Edward Is. and Magdalen Is. (Figure 7, Figure 8, August). Occurrence levels remain high in September, but the seasonal decrease slowly begins, while station A peaks and notable levels persist at station G West of Anticosti Is. (Figure 7, Figure 8, September). The seasonal occurrence levels peak at this latter station in October, where proportions of occurrence exceeds 25% of the days (Figure 8, October), while a decrease is continuing at the other stations. The decrease goes on in November, while the mean occurrence level at station 5 in Shediac trough still exceed 50% (Figure 7, November), and only a few stations have occurrences in December (Figure 7, December).

In summary, the average spatial-temporal pattern observed over the PAM network is consistent with an immigration starting with a few rare NARW detections as early as April, with NARW upcall occurrences rapidly showing up in Southwestern Gulf. It is in May, however, that the proportion of days with NARW upcall occurrences indicate that the Gulf really starts to be colonized. This proportion of days with NARW upcall occurrences then grows and the general spatial pattern is maintained for the whole summer and fall. Significant proportion of days with NARW upcall occurrences are observed at all shelf- and shelf-edge stations, but with persistent highest levels in the Shediac trough. The incursion phase from these PAM observations culminates in August, before reverting to a retreat phase until the disappearance of NARW upcall detection in December, except for a few rare occurrences. Meanwhile, the proportion of days with NARW upcall occurrence in the area northwest of Anticosti Is. follows the same seasonal pattern as the Southwestern Gulf, but at a lower level, with a start in May, maintenance of moderate levels all along the summer and fall, with somewhat higher levels in August and October.

NARW UPCALL SEASONAL OCCURRENCE PROPORTIONS AND IN / OUT FLOW

The cumulative proportion of days with NARW upcall occurrence over the annual cycle in Gulf of St. Lawrence was compiled by integrating the observations at the seafloor PAM stations network over 2015 to 2022, the period of steady seasonal NARW upcall occurrence (Figure 10 upper panel, blue line). This seafloor PAM dataset has observations over the entire year, in contrast to the Viking OOS buoy dataset, and the monthly effort is relatively even throughout the year (1,149 ± 53 (SE) d/m; 37.7 ± 1.7 (SE) d/Julian d) (Figure 10 upper panel, red line). Therefore the year-round cumulative proportion of occurrence curve (Figure 10 lower panel, blue line; Equation 7) is not dependent upon variations in the days with observations across the annual cycle, and the relative stability of the seasonal proportion of days with NARW upcall occurrence over the multi-year time series allows to interpret the curves as a proxy for the average seasonal NARW PAM occurrence within the whole Gulf.

For example, the time when 2.5% of the annual sum of the daily ratios of NARW upcall occurrence arises is 25 May (Table 4). The time window of the bulk of the occurrence (50% of annual sum) is between 16 July and 18 September. The seasonal occurrence peaks on 17 August. The rate of change during the rising or the decreasing phases is non-monotonous (Figure 10, red line), but this could result from time-space variability in the observations (Figure 10, upper panel, red curve).

DISCUSSION

ALLEVIATION OF LIMITATIONS OF THE DATASET

The analyzed PAM data from 2010 to 2022 over 20 stations, representing a total of 65.8 years of days with observations, is among the big-data ensembles that today's technologies generate. Thanks to the early initiation of the data collection, this dataset accumulated a considerable amount of information allowing to track changes in the Gulf of St. Lawrence ecosystem at a decadal time scale, notably the tracking of the 2015 change in NARW use of the Gulf resources (Simard et al. 2019). The long-term data grouped in this report was acquired at the favor of several dedicated particular research projects and therefore was not systematically planned to embrace a monitoring over the whole Gulf of St. Lawrence. As a result, the sampling effort varied over the years and experienced a marked intensification of the coverage after the 2017 high NARW mortality event in the Gulf (Daoust et al. 2017). This variable sampling intensity over time and space of the analyzed dataset has to be carefully taken into account to avoid misinterpreting the results that might arise from non uniform sampling. Similarly, the higher stationarity in time series of days with NARW upcall occurrences in the most frequented areas after 2015 (Figure 2) imposed the retention of only the post-2015 years segment for some analyses.

Other known particularities of PAM sampling in ocean ecosystems, where 3D propagation effects and variable signal-to-noise ratios affects the detection probability at a given measurement point (e.g. Davis et al. 2017; Gervaise et al. 2021; Simard et al. 2008; Simard et al. 2019; Simard et al. 2022), were largely damped by the choice of a coarse time-occurrence metric of days with presence of NARW upcall. A single call is then sufficient to get a positive day. This has the effect of enhancing the visibility and continuity of rare events, which must be kept in mind when interpreting the occurrence time series. Such effect is clearly visible in the time series of days with NARW upcall occurrence per week at station 2 (Figure 2). The use of a finer metric, such as the number of hours with NARW upcall per day in Simard et al. (2019) lowers the visibility and the continuity of NARW upcall occurrence at this station. Similarly, the 2015 change in NARW upcall occurrence in the Shediac trough basin varied by a factor of 3-4 for the proportion of days with NARW upcall presence to a factor > 10 for the number of detections or hours with NARW upcall per day (cf. tables 1 and 2 in Simard et al. 2019). This coarse data handling also reduces the possible small contribution to the variability that could result from the different recording systems used, whose characteristics were furthermore selected to get similar acoustic sensitivity. Similarly, the use of the day-with-presence metric minimizes possible effects of the know time-space variability in NARW calling rates (Davis et al. 2023; Franklin et al. 2022; Matthews et al. 2001; Matthews and Parks 2021; Parks et al. 2011). To optimize propagating NARW upcalls detectability, the 3D position of the data collection points were carefully selected within the core of the regional CIL sound propagation channel and away from the St. Lawrence seaway where merchant ships leave a detrimental noisy footprint in the frequency band of the NARW upcall (Simard et al. 2016). Their detection was then maximized by using the Ver. 2.0 of the NARW upcall CDNN AI-algorithm optimized for the Gulf of St. Lawrence ambient soundscape, which produced the highest recall and precision

performance indexes (cf. Appendix 2). The validation of all detections by one or two experts filtered out all the false alarms, including the similar upcalls from humpback whales (e.g. Appendix 3).

We are therefore confident that the information presented here on the mesoscale habitat use by NARW in the St. Lawrence ecosystem throughout the annual cycle since 2015 is robust to the limitations of the analyzed dataset and possible bias arising from methodological handling of the inherent multi-scale spatial and temporal variability.

THE WHEN AND WHERE OF THE NARW USE OF THE GULF OF ST. LAWRENCE

Despite the non-systematic or random sampling design and its limited number of stations, the seafloor PAM dataset offers a reasonable coverage of all regions of the Gulf of St. Lawrence and Lower Estuary, with an emphasis in areas of high NARW occurrences, for the post-2015 time period of their steady frequentation of this ecosystem during the ice-free season. The portrait of NARW use of this particular productive habitat of the Northwest Atlantic can be summarized by the following time space pattern over an average annual cycle.

1. During winter, except for very rare occurrences, NARW upcalls were not detected, which does not support significant NARW presence in the Gulf during this period.
2. The first signs of upcall occurrence start in April, on the Southwestern shelf and slope of the Laurentian Channel, including the southeastern tip of Anticosti Is.
3. At the beginning of May, a first and most intensive wave of NARW incursion into the Gulf is taking place and last for ~ 1.5 month. On May 27th, 2.5% of the cumulated annual occurrence is reached; 5% on June 8th. The NARW occurrence input is followed by a second wave in the first half of July, at which time 25% of the cumulated annual occurrence is reached (July 17th). The occurrence continues to increase at a slower pace until mid-August.
4. During the above incursion period, the Southwestern shelf is colonized and the maximal occurrences are located into the Shediac trough. A secondary area of lower occurrence northwest of Anticosti Is. follows a similar temporal colonization pattern.
5. This general spatial pattern of NARW occurrence persists while the retreat goes on at a constant rate up to mid-October, before the decrease in occurrence is slowed down for ~ 1 month.
6. Five percent (5%) of the observed days with NARW upcalls occur after November 1st; 2.5% after November 20th.
7. In December the retreat is essentially completed, and only rare occurrences are observed at a few stations.
8. During the seasonal occurrence period, there is a considerable variability around the mean occurrence rate at the stations, within a season and across seasons.

ACKNOWLEDGEMENTS

This work was realized with supports from Fisheries and Oceans Canada (DFO), NSERC Discovery and Canadian Foundation for Innovation grants to YS and the DFO Research Chair in underwater acoustics applied to marine mammals at UQAR-ISMER. We are grateful to all people and crews who participated to the data collection at sea, their analysis in the laboratory, managers and collaborators, without whom the success of this multi-partner and multi-disciplinary research would not have happened.

REFERENCES CITED

Aulanier, F., Simard, Y., Lebel, P., Mercure-Boissonneau, P., and Philippe, E. 2021. Atlas des paysages acoustiques océaniques / *Ocean Soundscape Atlas*. [accessed 2024-02-05.

Brillant, S.W., Vanderlaan, A.S.M., Rangeley, R.W., and Taggart, C.T. 2015. Quantitative estimates of the movement and distribution of North Atlantic right whales along the northeast coast of North America. Endang. Sp. Res. 27(2): 141-154. [accessed 2024-02-05].

Cooke, J.G. 2020. *Eubalaena glacialis* (errata version published in 2020). The IUCN Red List of Threatened Species 2020: e.T41712A178589687: 18 p.

COSEWIC. 2013. COSEWIC assessment and status report on the North Atlantic Right Whale *Eubalaena glacialis* in Canada. Committee on the Status of Endangered Wildlife in Canada., Ottawa: xi + 58 pp.

Crowe, L., Brown, M.A., Corkeron, P., Hamilton, P., Ramp, C., Ratelle, S., Vanderlaan, A., and Cole, T. 2021. In plane sight: a mark-recapture analysis of North Atlantic right whales in the Gulf of St. Lawrence. Endanger. Sp. Res. 46: 227-251.

Daoust, P.-Y., Couture, E.L., Wimmer, T., and Bourque, L. 2017. Incident Report: North Atlantic right whale mortality event in the Gulf of St. Lawrence, 2017. Collaborative Report Produced by: Canadian Wildlife Health Cooperative and Marine Animal Response Society, and Fisheries and Oceans Canada.

Davis, G.E., Baumgartner, M.F., Bonnell, J.M., Bell, J., Berchok, C., Bort Thornton, J., Brault, S., Buchanan, G., Charif, R.A., Cholewiak, D., Clark, C.W., Corkeron, P., Delarue, J., Dudzinski, K., Hatch, L., Hildebrand, J., Hodge, L., Klinck, H., Kraus, S., Martin, B., Mellinger, D.K., Moors-Murphy, H., Nieukirk, S., Nowacek, D.P., Parks, S., Read, A.J., Rice, A.N., Risch, D., Širović, A., Soldevilla, M., Stafford, K., Stanistreet, J.E., Summers, E., Todd, S., Warde, A., and Van Parijs, S.M. 2017. Long-term passive acoustic recordings track the changing distribution of North Atlantic right whales (*Eubalaena glacialis*) from 2004 to 2014. Sci. Rep. 7(1): 13460.

Davis, G.E., Tennant, S.C., and Van Parijs, S.M. 2023. Upcalling behaviour and patterns in North Atlantic right whales, implications for monitoring protocols during wind energy development. ICES J. Mar. Sci.

DCLDE. 2013. The 6th International Workshop on Detection, Classification, Localization, and Density Estimation (DCLDE) of Marine Mammals using Passive Acoustics. [accessed 4 Feb. 2024].

DFO. 2014. Recovery Strategy for the North Atlantic Right Whale (*Eubalaena glacialis*) in Atlantic Canadian Waters [Final]. Species at Risk Act Recovery Strategy Series Fisheries and Oceans Canada., Ottawa, Ontario: vii +68 pp.

Franklin, K. J., Cole, T. V. N., Cholewiak, D. M., Duley, P. A., Crowe, L. M., Hamilton, P. K., Knowlton, A. R., Taggart, C. T., Johnson, H. D. et al. 2022. Using sonobuoys and visual surveys to characterize North Atlantic right whale (*Eubalaena glacialis*) calling behavior in the Gulf of St. Lawrence. Endang. Sp. Res. 49**:** 159-174.

Galbraith, P.S., Chassé, J., Shaw, J.-L., Dumas, J., Lefaivre, D., and Bourassa, M.-N. 2023. Physical oceanographic conditions in the Gulf of St. Lawrence during 2022. Can. Tech. Rep. Hydrogr. Ocean Sci. Fisheries and Oceans Canada: v + 88 p.

Gervaise, C., Simard, Y., Aulanier, F., and Roy, N. 2019a. Optimal passive acoustic systems for real-time detection and localization of North Atlantic right whales in their feeding ground off Gaspé in the Gulf of St. Lawrence. Can. Tech. Rep. Fish. Aquat. Sci. 3345: ix + 58 pp.

Gervaise, C., Simard, Y., Aulanier, F., and Roy, N. 2019b. Performance study of passive acoustic systems for detecting North Atlantic right whales in seaways: the Honguedo strait in the Gulf of St. Lawrence. Can. Tech. Rep. Fish. Aquat. Sci. 3346: ix + 53 pp.

Gervaise, C., Simard, Y., Aulanier, F., and Roy, N. 2021. Optimizing passive acoustic systems for marine mammal detection and localization: Application to real-time monitoring north Atlantic right whales in Gulf of St. Lawrence. Appl. Acoust. 178: 107949.

Kirsebom, O.S., Frazao, F., Simard, Y., Roy, N., Matwin, S., and Giard, S. 2020. Performance of a deep neural network at detecting North Atlantic right whale upcalls. J. Acoust. Soc. Am. 147(4): 2636-2646.

Kraus, S.D., and Rolland, R.M. 2007. Right whales in the urban ocean. *In* The urban whale. *Edited by* S.D. Kraus and R.M. Rolland. Cambridge, MA: Harvard. pp. 1-39.

Linden, D.W. 2023. Population size estimation of North Atlantic right whales from 1990-2022. US Dept. Commer. Northeast Fish. Sci. Center NOAA Tech. Memo. NMFS-NE-314: 14 p.

Matthews, J.N., Brown, S., Gillespie, D., Johnson, M., McLanaghan, R., Moscrop, A., Nowacek, D., Leaper, R., Lewis, T., and Tyack, P. 2001. Vocalisation rates of the North Atlantic right whale (*Eubalaena glacialis*). J. Cetacean Res. Manag. 3(3): 271-282.

Matthews, L.P., and Parks, S.E. 2021. An overview of North Atlantic right whale acoustic behavior, hearing capabilities, and responses to sound. Mar. Poll. Bull. 173: 113043.

Meyer-Gutbrod, E.L., Greene, C.H., Davies, K.T.A., and Johns, D.G. 2021. Ocean regime shift is driving collapse of the North Atlantic right whale population. Oceanography 34(3): 22-31.

Parks, S.E., and Tyack, P.L. 2005. Sound production by North Atlantic right whales (*Eubalaena glacialis)* in surface active groups. J. Acoust. Soc. Am. 117(5): 3297-3306.

Parks, S.E., Urazghildiiev, I., and Clark, C.W. 2009. Variability in ambient noise levels and call parameters of North Atlantic right whales in three habitat areas. J. Acoust. Soc. Am. 125(2): 1230-1239.

Parks, S.E., Johnson, M., Nowacek, D., and Tyack, P.L. 2011. Individual right whales call louder in increased environmental noise. Biol. Lett. 7: 33-35.

Plourde, S., Lehoux, C., Johnson, C.L., Perrin, G., and Lesage, V. 2019. North Atlantic right whale (*Eubalaena glacialis*) and its food: (I) a spatial climatology of Calanus biomass and potential foraging habitats in Canadian waters. J. Plankt. Res. 41(5): 667-685.

Record, N.R., Runge, J.A., Pendleton, D.E., Balch, W.M., Davies, K.T.A., Pershing, A.J., Johnson, C.L., Stamieszkin, K., Ji, R., Feng, Z., Kraus, S.D., Kenney, R.D., Hudak, C.A., Mayo, C.A., Chen, C., Salisbury, J.E., and Thompson, C.R.S. 2019. Rapid climate-driven circulation changes threaten conservation of endangered North Atlantic right whales. Oceanography 32: 162−169.

Roberts, J. J., Yack, T. M. , Fujioka, E., Halpin, P. N., Baumgartner, M. F., Boisseau, O.. et al. 2024. North Atlantic right whale density surface model for the US Atlantic evaluated with passive acoustic monitoring. Mar. Ecol. Prog. Ser. 732: 167-192.

Simard, Y., Roy, N., and Gervaise, C. 2008. Passive acoustic detection and localization of whales: Effects of shipping noise in Saguenay–St. Lawrence Marine Park. J. Acoust. Soc. Am 123(6): 4109-4117.

Simard, Y., Roy, N., Gervaise, C., and Giard, S. 2016. Analysis and modeling of 255 source levels of merchant ships from an acoustic observatory along St. Lawrence Seaway. J. Acoust. Soc. Am. 140(3): 2002-2018.

Simard, Y., Roy, N., Giard, S., and Aulanier, F. 2019. North Atlantic right whale shift to the Gulf of St. Lawrence in 2015, revealed by long-term passive acoustics. Endang. Sp. Res. 40: 271-284.

Simard, Y., Duquette, K., Royer, P., Roy, N., Rousseau, M., Juif, C., Gervaise, C., and Constans, C. 2022. Large circular hydrophone arrays for long-range monitoring of North Atlantic right whales: first deployments and testing in the Gulf of St. Lawrence. Can. Tech. Rep. Fish. Aquat. Sci. 3491: viii + 40 p.

Winn, H.E., Price, C.A., and Sorensen, P.W. 1986. The distributional biology of the right whale (*Eubalaena glacialis)* in the Western North Atlantic. Reports - International Whaling Commission, Special Issue 10: 129-138.

FIGURES

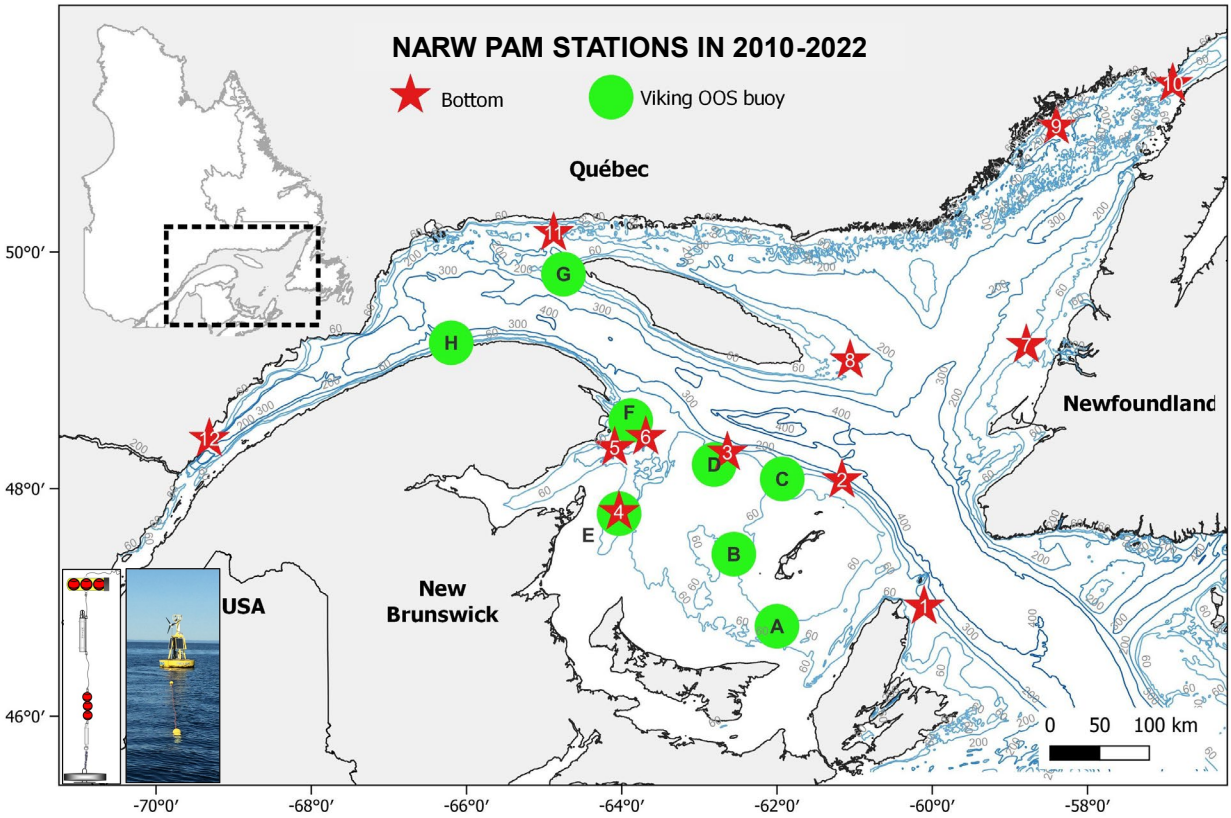

Figure 1. Bathymetric map of the Estuary and Gulf of St. Lawrence in eastern Canada showing locations of the stations where PAM systems were deployed with demersal I-moorings (stars with numbers, scheme) or from the Viking OOS surface buoys (circles with letters, photo) with hydrophones at a depth of ~25 m. Station labels are ordered with traveling distance from Cabot strait.

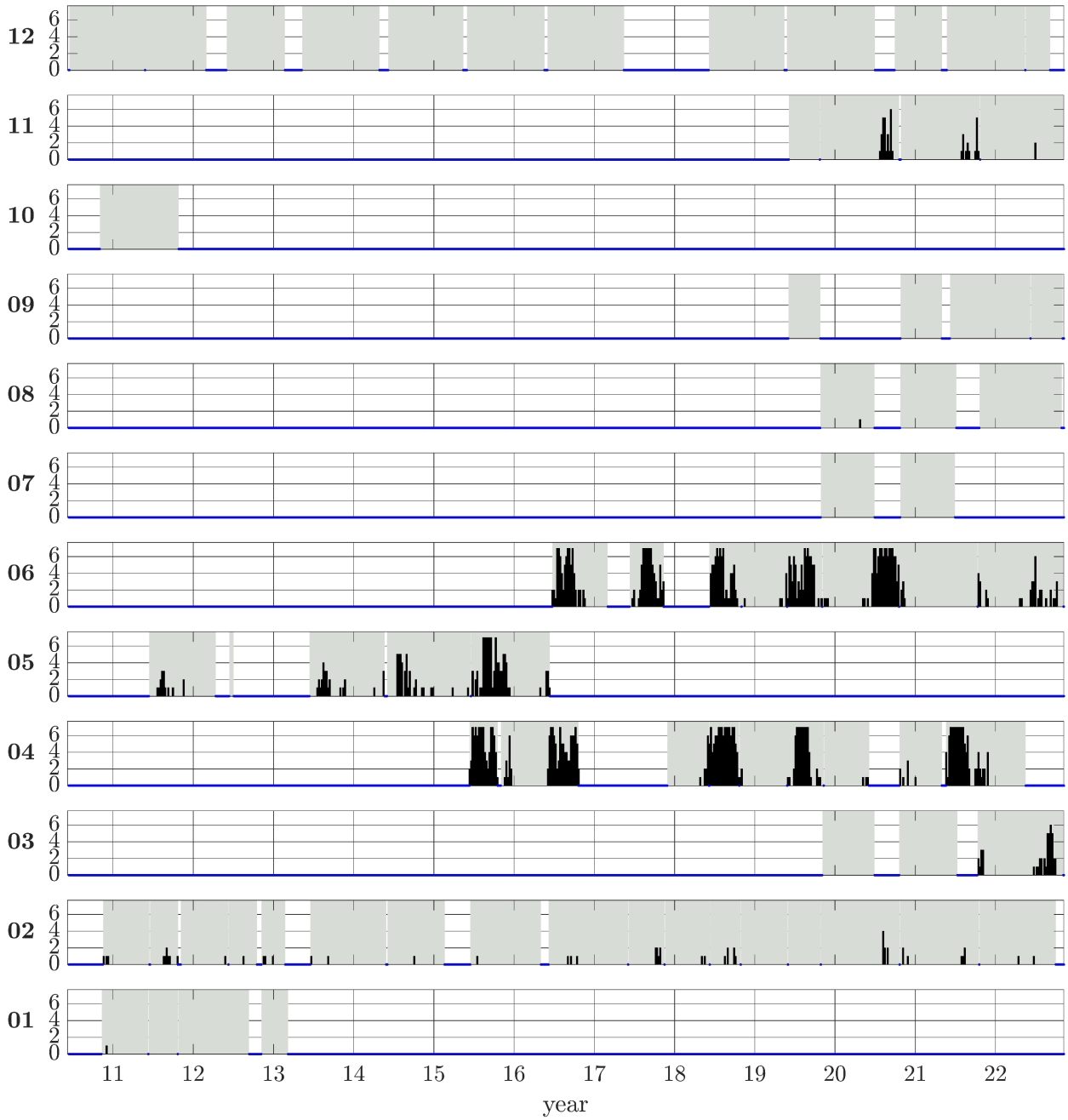

Figure 2. Number of days with NARW upcalls per week, $d_7(s,w)$ (Eq. 1), from 2010 to 2022 at the seafloor stations, ordered from distance to Cabot strait. Shaded areas indicate observation periods.

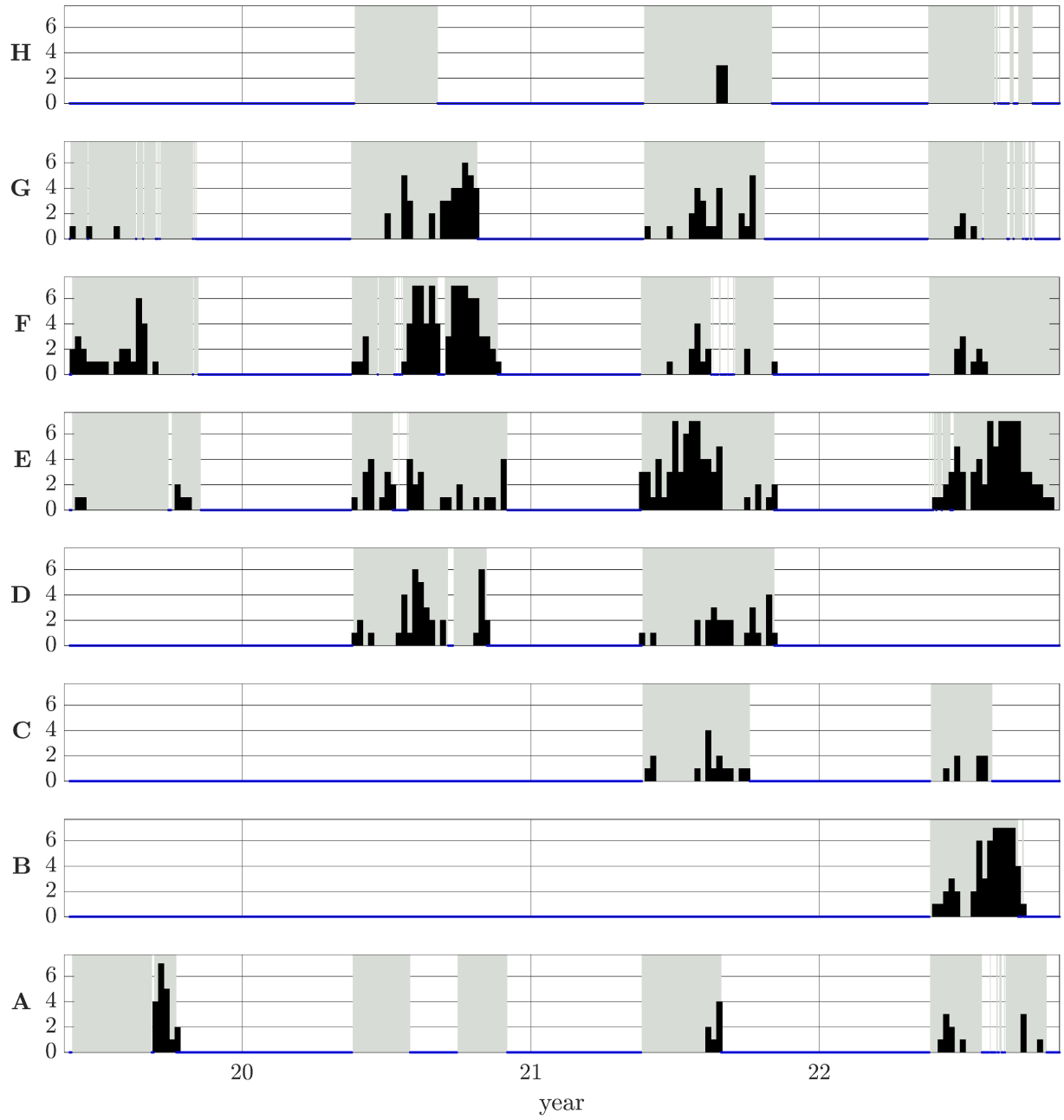

Figure 3. Number of days with NARW upcalls per week, $d_7(s,w)$ (Eq. 1), from 2019 to 2022 at the Viking OOS stations, ordered from distance to Cabot strait. Shaded areas indicate observation periods. Note. Exceptionally, the results presented for station H in 2020 were obtained using the CDNN AI-algorithm Ver. 1.0 on real-time recordings, in contrast to the rest of the data, where the processing with the CDNN AI-algorithm Ver. 2.0 was done post-acquisition, on the data files stored in the memory of the acquisition systems.

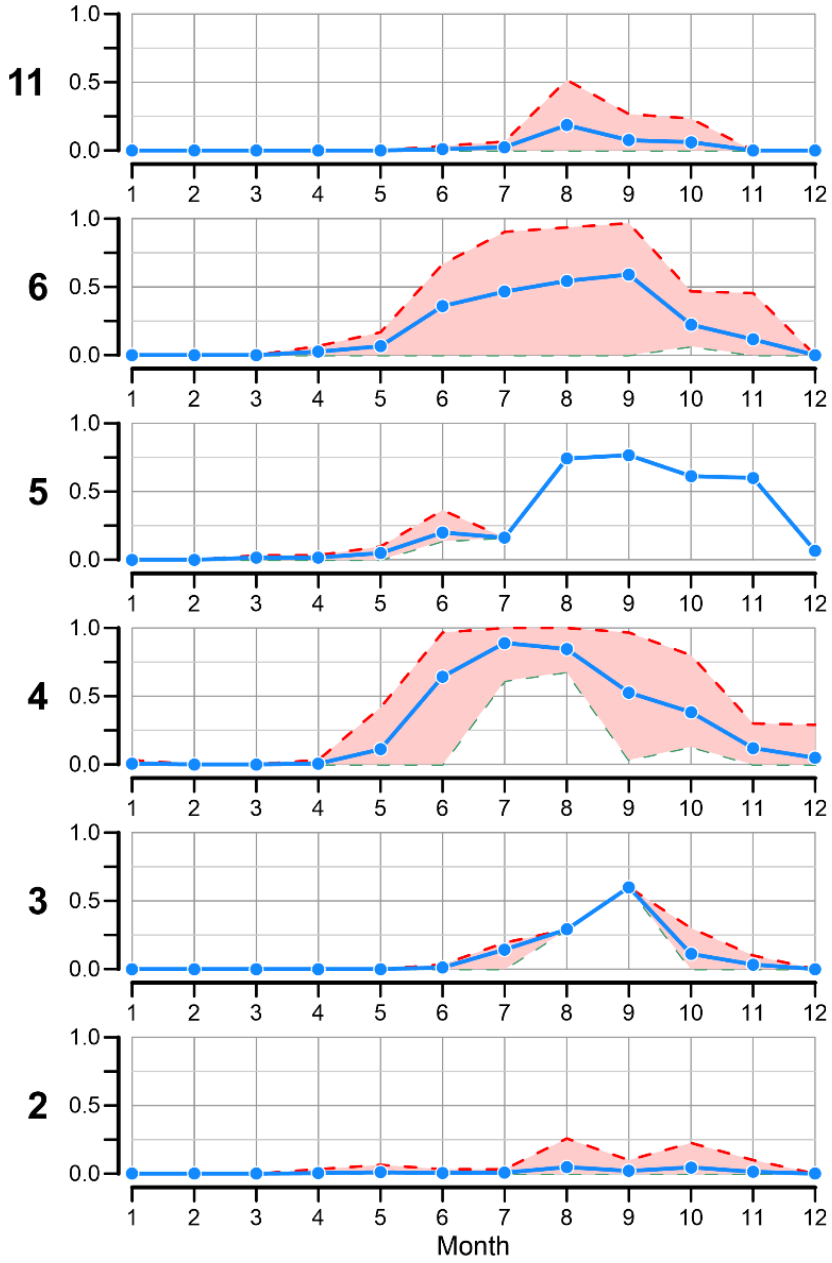

Figure 4. Monthly proportion of days of observation with NARW upcalls at the seafloor PAM stations of frequent occurrence during 2015 to 2022, ordered with distance from Cabot strait. Dotted blue line: $p_n(R,m)$, (Eq. 4a) ; dashed red line: maximum year, $max\ (p_n(R,y,m))$ (Eq. 5); dashed green line: minimum year, $min\ (p_n(R,y,m)$, (Eq. 5); Pink envelope: [min, max] range.

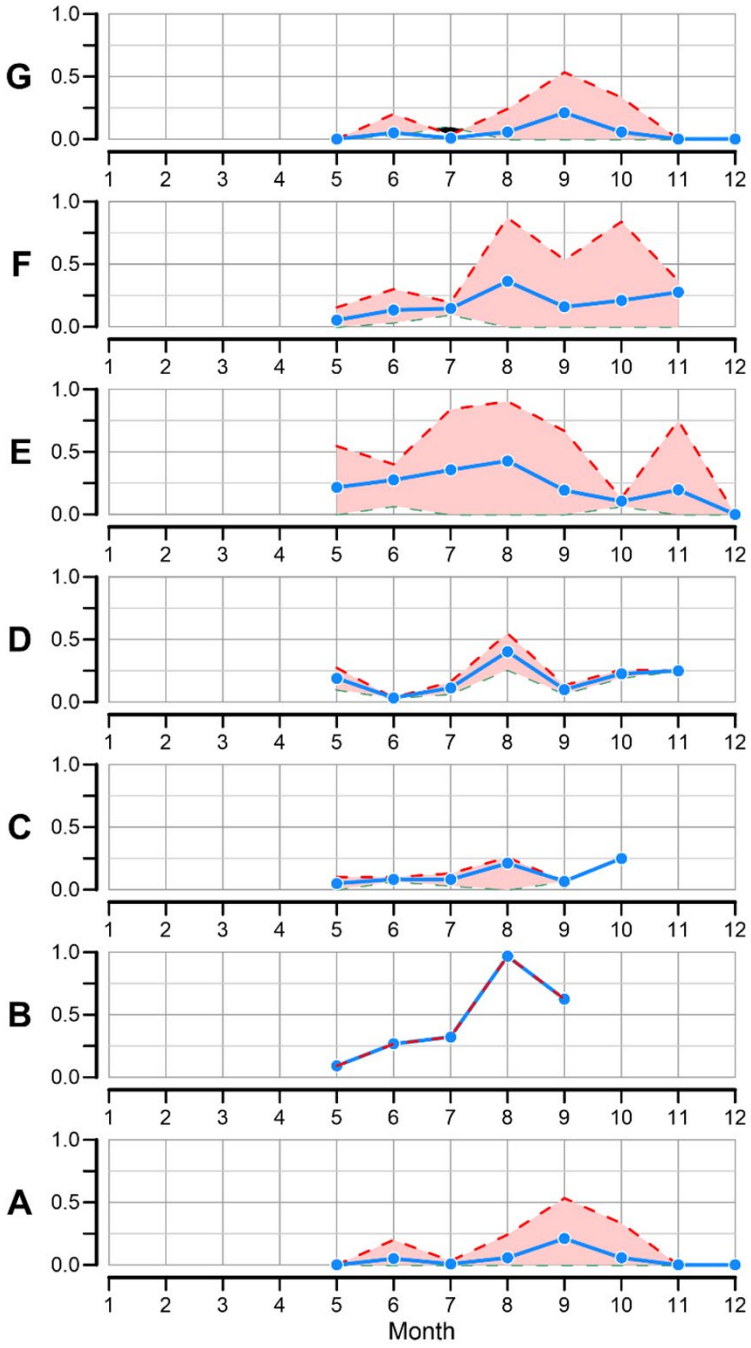

Figure 5. Proportion of days of observation with NARW upcalls per month during 2019 to 2022 at the Viking OOS stations of frequent occurrence, ordered with distance from Cabot strait. Dotted blue line: $p_n(R,m)$, (Eq. 4b) ; dashed red line: maximum year, $max\ (p_n(R,y,m))$ (Eq. 5); dashed green line: minimum year, $min\ (p_{nd}(R,y,m)$, (Eq. 5); Pink envelope: [min, max] range.

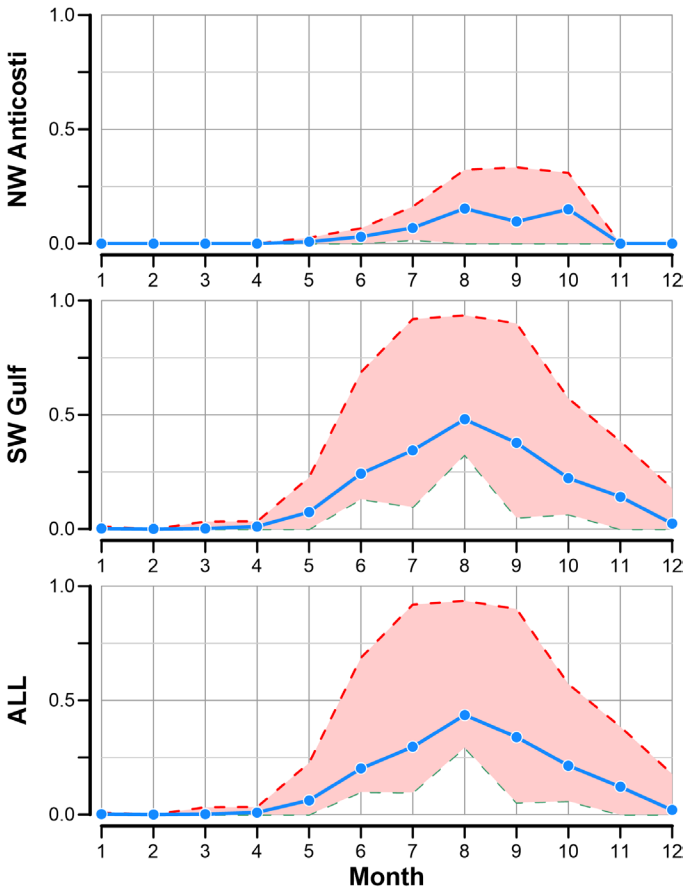

Figure 6. Proportion of days of observation with NARW upcalls per month during 2015 to 2022 in Southwest Gulf of St. Lawrence from the Viking buoys and the seafloor Pam datasets (stations A-F + 3-6), Northwest Anticosti (stations G + 11) and stations from both regions pooled together. Legend as in figures 4 and 5, but for stations grouped by region as indicated.
Note: NW Anticosti stations began in 2019, while SW Gulf began in 2015.

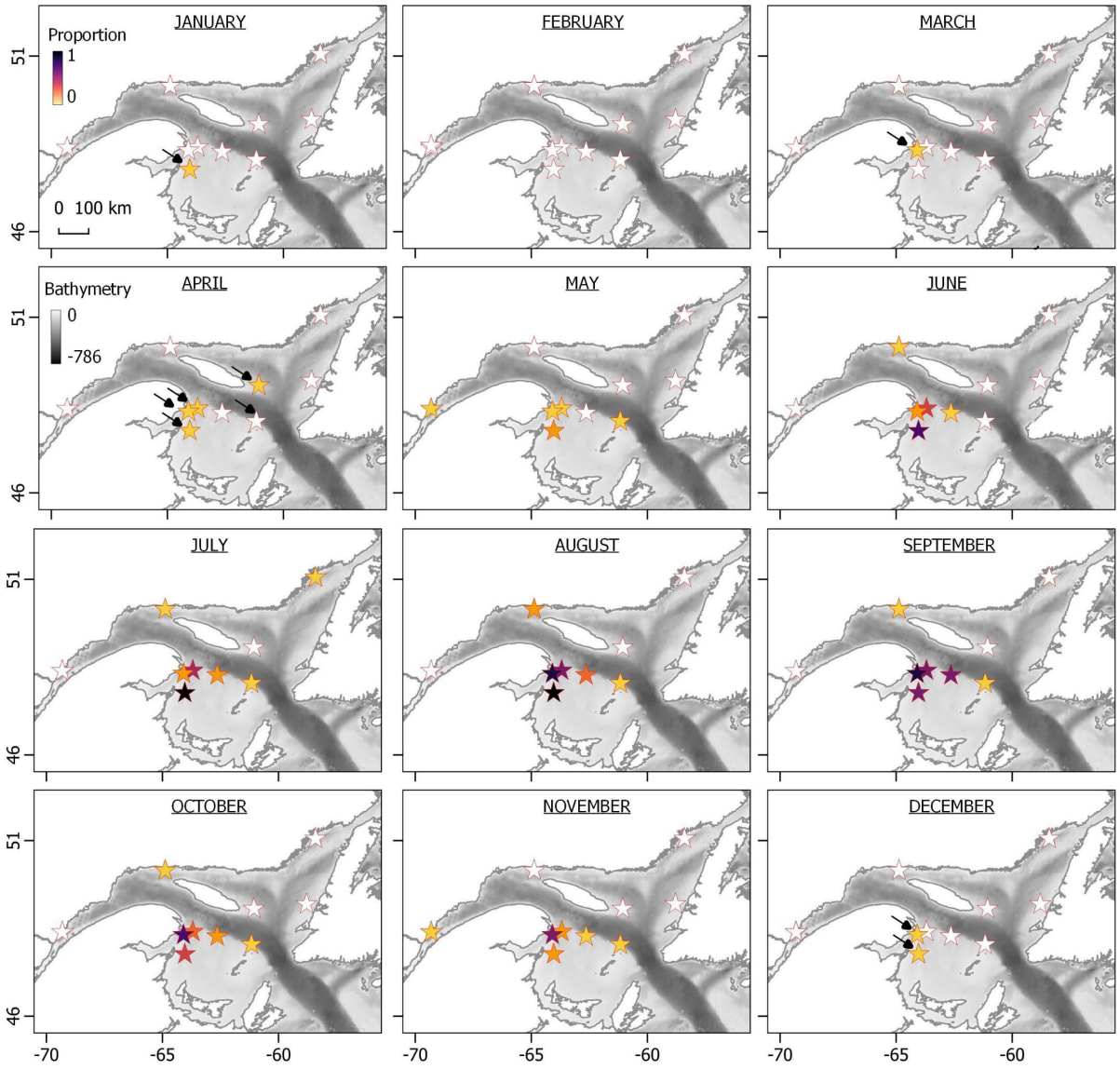

Figure 7. Monthly maps of the average proportion of days of observation with NARW upcalls in Gulf of St. Lawrence over 2015 to 2022 from the seafloor PAM network, $p_n(s,m)$, (Eq. 3a). Gray hatching: bathymetry in meters.

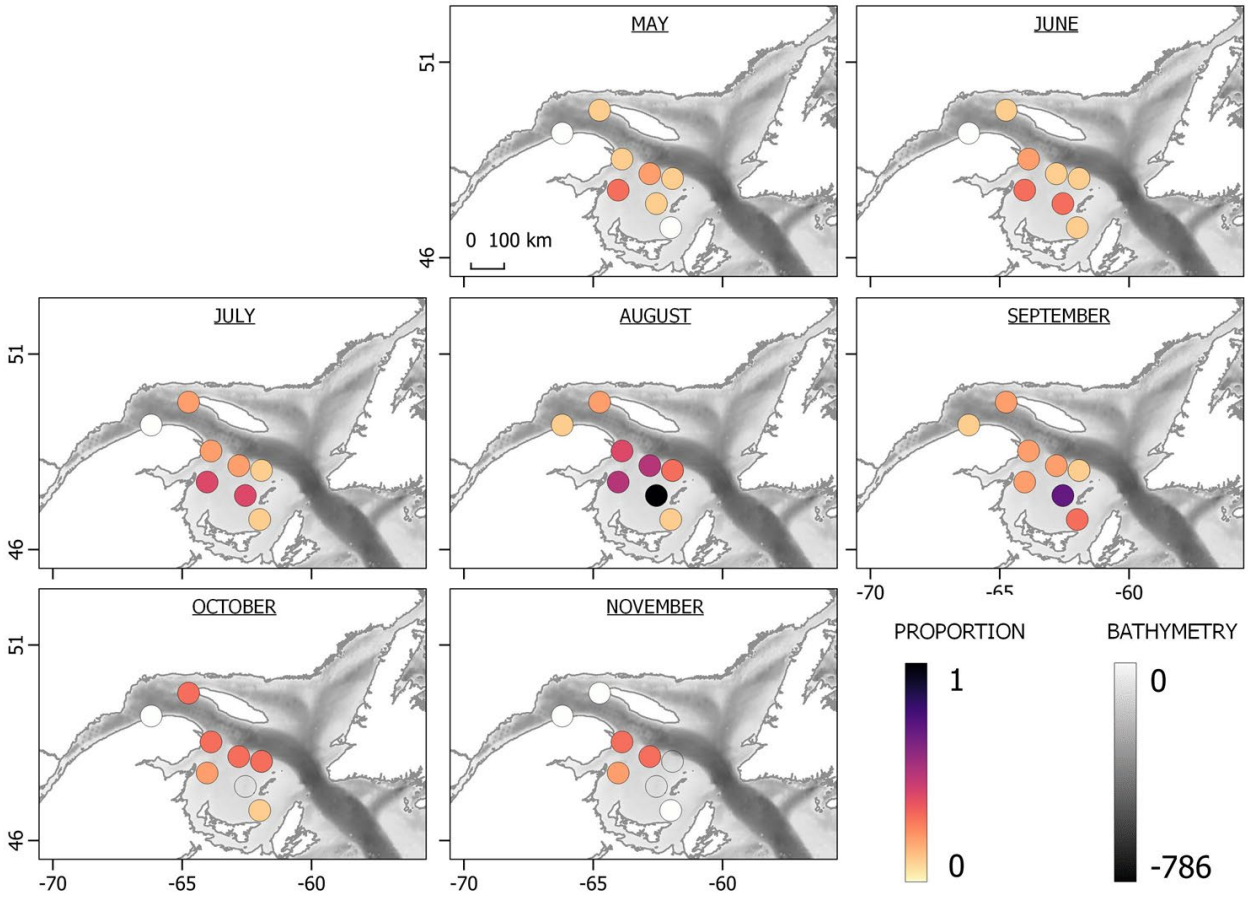

Figure 8. Monthly maps of the average proportion of days of observation with NARW upcalls in Gulf of St. Lawrence over 2019 to 2022 from the Viking OOS buoy network, p_n (s, m), (Eq. 3b). Gray hatching: bathymetry in meters.

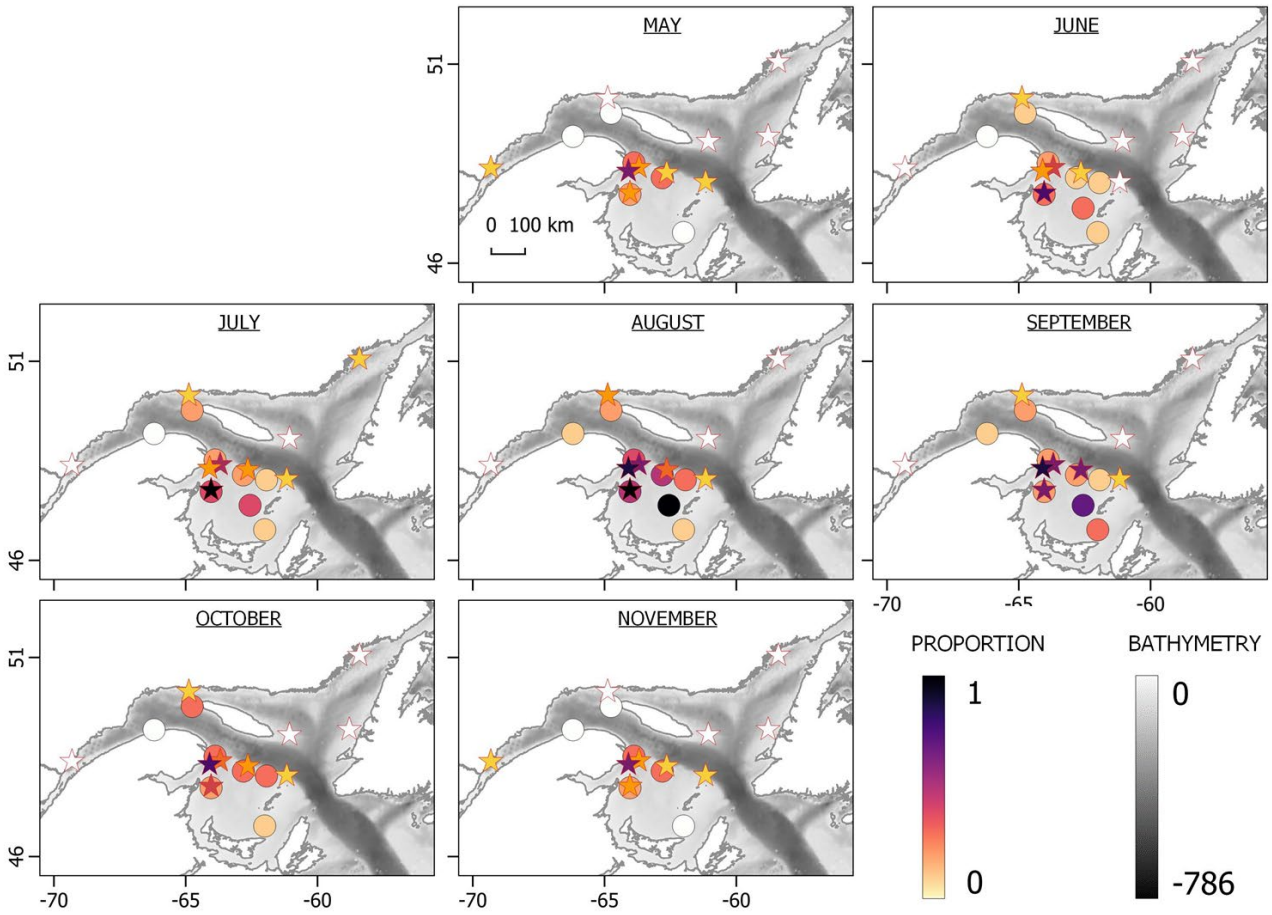

Figure 9. Monthly maps of the average proportion of days of observation with NARW upcalls (in Gulf of St. Lawrence over 2015 to 2022 from the Viking OOS buoy network (circles), p_n (s,m), (Eq. 3b), and the seafloor PAM network (stars) p_n (s, m), (Eq. 3a). Gray hatching: bathymetry in meters.

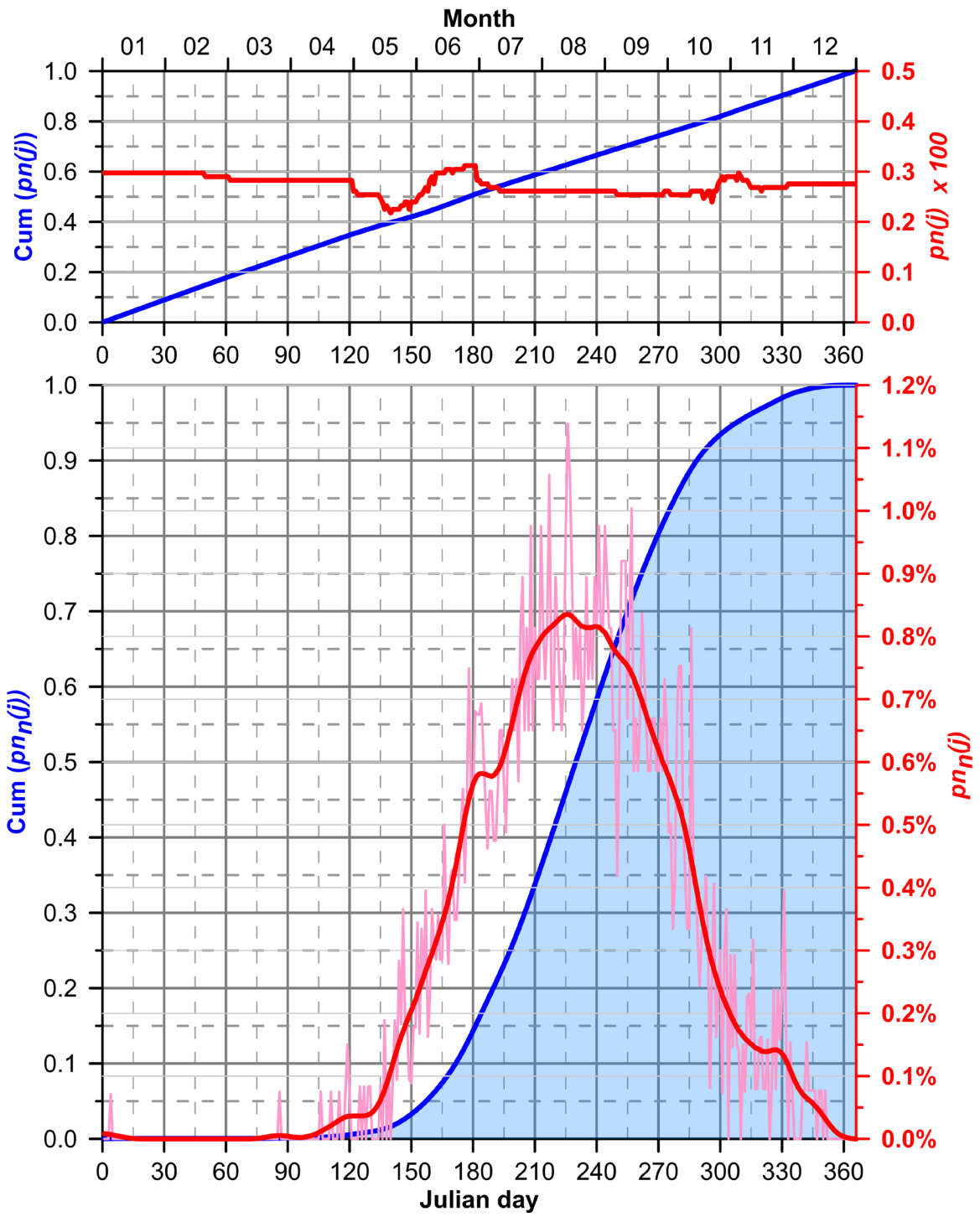

Figure 10. Lower panel: Probability distribution (pdf) and cumulative probability distribution (cdf) of mean daily proportion of days of observation with NARW upcalls over the annual cycle, cdf of (pn_n (j)) (Eq. 7) (blue shading), pdf of pn_n (j) (pink line) and filtered (28-d Gaussian) pn_n (j) (bold red line) in Gulf of St. Lawrence from the seafloor PAM stations network over 2015 to 2022. Upper panel: corresponding proportions of days of observations, (pn (j)), over the PAM network (Eq. 8).

TABLES

Table 1. Coordinates of the PAM stations deployed from seafloor I-type moorings.*

Station	Name	Latitude	Longitude	Bottom depth (m)	Years	Effort (d)	NARW (d)	NARW %
12	Escoumins	48° 23.66' N	69° 18.84' W	136	2010-2022	3726	0	0
11	Riv.-au-Tonnerre	50° 07.54' N	64° 52.64' W	121	2019-2022	1551	43	2.8
10	Belle-Isle	51° 20.49' N	56° 54.04' W	110	2010-2011	358	0	0
9	Mécatina	50° 59.95' N	58° 24.01' W	100	2019-2022	1203	0	0
8	Anticosti East	49° 03.69' N	61° 03.40' W	90	2019-2022	1081	1	0.1
7	Bonne Bay shelf	49° 11.48' N	58° 47.21' W	106	2019-2021	496	0	0
6	Percé	48° 24.68' N	63° 41.40' W	109	2016-2022	2218	482	21.7
5	Cap d'Espoir	48° 19.13' N	64° 05.46' W	87	2011-2016	1411	183	13.0
4	Shediac	47° 45.90' N	64° 02.05' W	83	2016-2022	2133	534	25.0
3	Orphelin	48° 16.67' N	62° 38.30' W	103	2019-2021	1251	44	3.5
2	Old Harry	48° 02.47' N	61° 09.73' W	103	2010-2022	4392	54	1.2
1	Cabot	46° 56.40' N	60° 06.24' W	131	2010-2013	794	1	0.1
					Total :	20614	1342	6.5

*Locations of last-year deployments.

Table 2. Coordinates of the PAM stations deployed from the Viking OOS surface buoys.*

Station	Name	Latitude	Longitude	Bottom depth (m)	Years	Effort (d)	NARW (d)	NARW %
H	IML-7 Gaspé current (CG)	49° 14.53' N	66° 11.80' W	183	2019-2022	378	6	1.6
G	IML-13 Banc Parent (BP)	49° 49.00' N	64° 44.99' W	108	2019-2022	589	73	12.4
F	IML-11 Banc des américains (BA)	48° 35.00' N	63° 53.00' W	163	2019-2022	635	134	21.1
E	IML-6 Shediac valley (VAS)	47° 47.00' N	64° 02.00' W	83	2019-2022	663	183	27.6
D	IML-14 Orphelin	48° 12.44' N	62° 48.51' W	80	2020-2022	329	62	18.8
C	IML-15 Anticosti-Est	48° 05.00' N	61° 55.90' W	69	2021-2022	214	22	10.3
B	IML-16 Eastern Bradelle (BB)	47° 25.92' N	62° 33.32' W	73	2022-2022	114	59	51.8
A	IML-12 East Southern Gulf (ESG)	46° 48.00' N	61° 59.98' W	73	2019-2022	491	37	7.5
					Total :	3413	576	16.9

* Locations of 2023 deployments.

Table 3. Acoustic instruments and settings used at the two sets of stations.

PAM set	Acoustic recorder
Seafloor	AURAL M2[a] with HTI-96 min hydrophone[b], 16-bit digitization, 16-dB recorder gain. Receiving sensitivity (RS) (including the 36-dB hydrophone preamp gain): -165 re 1 V/µPa over [0- 5 kHz] AMAR G4[c] with GeoSpectrum M36-C35-100 hydrophone with 35-dB preamp[d], 24-bit digitization, 16-dB recorder gain. Receiving sensitivity (RS) (including the 35-dB hydrophone preamp gain): -165 dB re 1 V/µPa over [0- 5 kHz] RTsys RESEA[e] with CO.L.MAR GP1190 hydrophone[f], 24-bit digitization, no recorder gain. Receiving sensitivity (RS) (no hydrophone preamp gain): -172 dB re 1 V/µPa over [0- 5 kHz]
Viking OOS	Ocean Sonic, icListen 24-bit digital hydrophone HF[g] Receiving sensitivity (RS) (no hydrophone preamp gain): -169 ± 1 dB re 1 V/µPa over [0- 5 kHz]

[a] Multi-electronique, Autonomous Underwater Acoustic Recorder for Acoustic Listening Model 2

[b] High-Tech Inc., HTI-96 min hydrophone

[c] Jasco Applied Sciences, Autonomous Multichannel Acoustic Recorder Generation 4

[d] GeoSpectrum Technologies Inc., hydrophone

[e] RTsys, RESEA hydrophone

[f] CO.L.MAR, GP1190 hydrophone

[g] Ocean Sonics, icListen HF smart hydrophone

Table 4. Time windows of NARW occurrence in the Gulf of St. Lawrence over the annual cycle and median occurrence date extracted from the cumulative probability distribution of days of observation with NARW occurrence on the seafloor PAM stations network between 2015 and 2022 (cf. Figure 10)

Proportion of annual occurrence	Start date	End date
95%	25 May	19 November
90%	5 June	2 November
50%	16 July	18 September
median	17 August	

APPENDIX 1

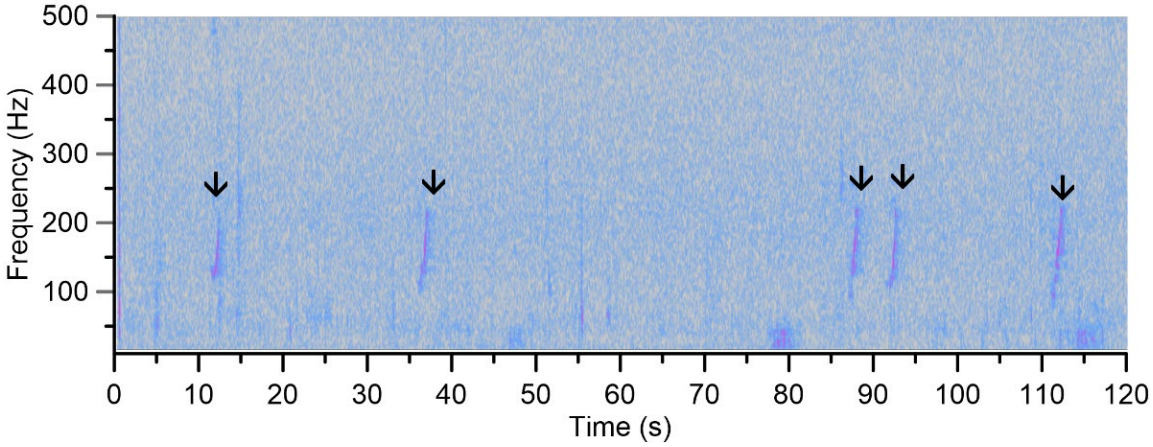

Figure 11. Examples of [10-500 Hz] spectrograms of NARW upcalls (arrows), recorded at station 4 in Shediac valley on 2021-08-02. Hanning window, resolution 0.26 s x 3.9 Hz.

APPENDIX 2

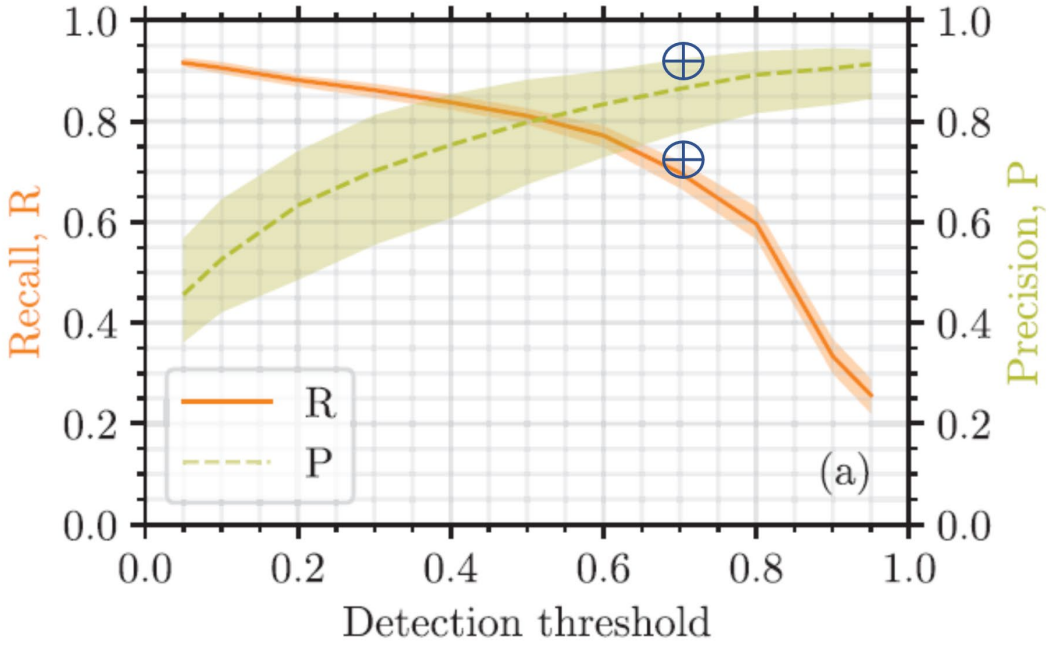

*Figure 12. Detection performance of the CDNN-AI algorithm for NARW upcalls Ver. 2.0 (⊕) used in the present report superimposed on the operational curves for the recall (R) and precision *(P)performance indexes of Ver. 1.0 estimated with the same test dataset (Kirsebom et al. 2020, Fig. 8a). The lines shows the average performance while the shaded bands show the 10% and 90% percentiles of the distribution of several iterations.*

APPENDIX 3

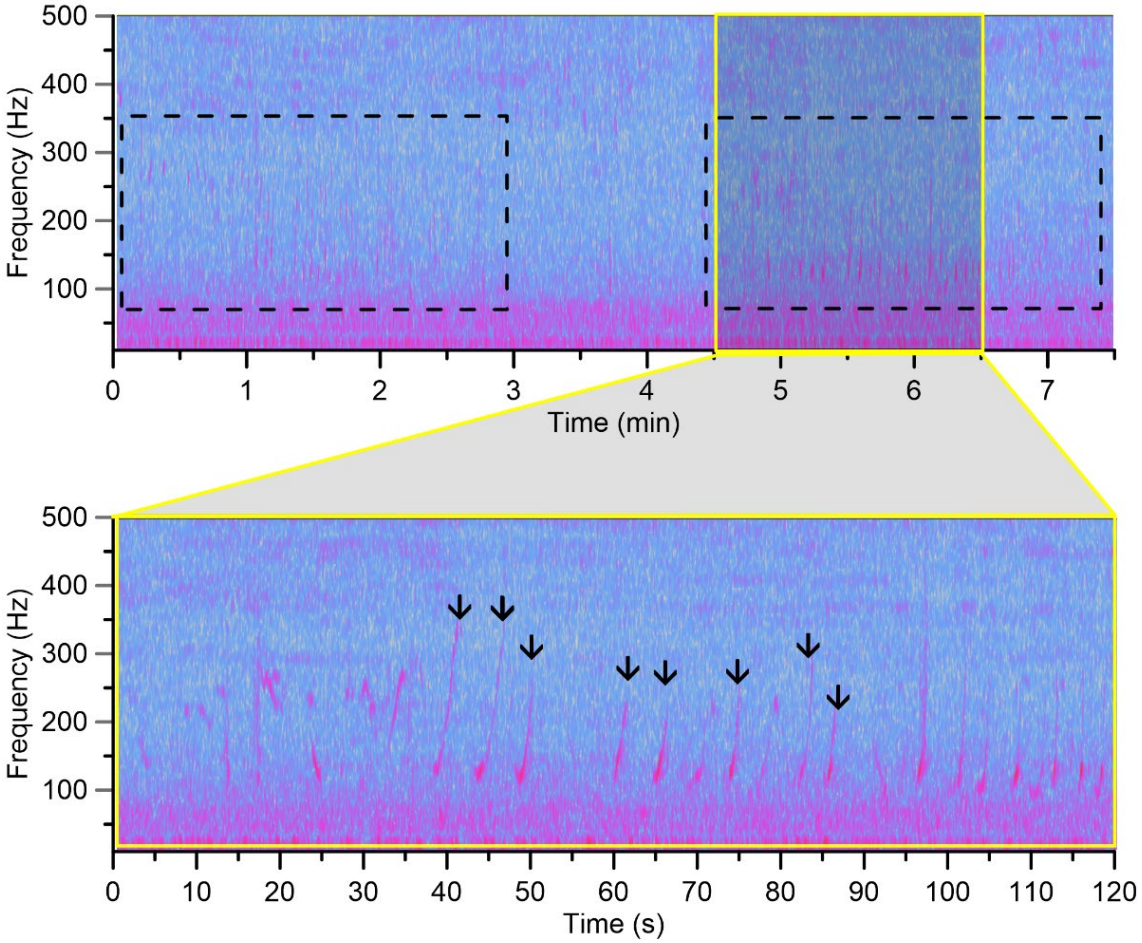

Figure 13. Examples of [10-500 Hz] spectrograms of humpback whale songs (upper panel, dashed lines rectangles) integrating series of upcalls (bottom panel zoom, arrows) alike NARW upcalls, recorded at station 1 in Cabot strait on 2010-11-11. Hanning window, resolution 0.25 s x 4 Hz.